JOURNAL OF AGRICULTURAL AND FOOD CHEMISTRY

pubs.acs.org/JAFC Article

Establishment of a Novel Cell Surface Display Platform Based on Natural "Chitosan Beads" of Yeast Spores

Zijie Li,*[,§] Wanjie Li,[§] Yasen Wang, Zhou Chen, Hideki Nakanishi, Xiangyang Xu, and Xiao-Dong Gao*

Cite This: J. Agric. Food Chem. 2022, 70, 7479−7489 Read Online

ACCESS | Metrics & More | Article Recommendations | Supporting Information

ABSTRACT: Cell surface display technology, which expresses and anchors proteins on the surface of microbial cells, has broad application prospects in many fields, such as protein library screening, biocatalysis, and biosensor development. However, traditional cell surface display systems have disadvantages: the molecular weight of phage display proteins cannot be too large; bacterial display lacks the post-translational modification process for eukaryotic proteins; yeast display is prone to excessive protein glycosylation and misfolding of multisubunit proteins; and the compatibility of *Bacillus subtilis* spore display needs to be further improved. Therefore, it is extremely valuable to develop an efficient surface display platform with strong universality and stress resistance properties. Although yeast surface display systems have been extensively investigated, the establishment of a surface display platform using yeast spores has rarely been reported. In this study, a novel cell surface display platform based on natural "chitosan beads" of yeast spores was developed. The target protein in fusion with the chitosan affinity protein (CAP) exhibited strong binding capability with "chitosan beads" of yeast spores *in vitro* and *in vivo*. Moreover, this protein display system showed highly preferable enzymatic properties and stability. As an example, the displayed LXYL-P1-2-CAP demonstrated high thermostability and reusability (60% of the initial activity after seven cycles of reuse), high storage stability (75% of original activity after 8 weeks), and excellent tolerance to a concentration up to 75% (v/v) organic reagents. To prove the practicability of this surface display system, the semisynthesis of paclitaxel intermediate was demonstrated and its highest conversion rate was 92% using 0.25 mM substrate. This study provides a novel and useful platform for the surface display of proteins, especially for multimeric macromolecular proteins of eukaryotic origin.

KEYWORDS: *cell surface display, yeast spores, chitosan affinity protein, enzymatic properties, paclitaxel*

INTRODUCTION

Cell surface display is a recombinant technology that expresses and anchors the target protein on the surface of microbial cells. The displayed protein on the surface maintains a relatively independent spatial structure and biological activity.[1] This technique exhibits a wide range of applications in many fields, such as nanobody screening,[2,3] biocatalysis,[4−6] biosensor development,[7,8] aquaculture,[9] and environmental repair.[10−12] Compared with traditional whole-cell catalysis containing intracellular enzymes, the expression of enzymes on the cell surface is advantageous because transmembrane transport of the substrate and product is not needed, thereby reducing the mass transfer limitation and improving the catalytic efficiency.

Currently, the host cells for surface display are mainly concentrated in phage,[13−15] bacteria,[16−22] yeast,[6,23−29] and *Bacillus subtilis* spores.[30−34] However, any traditional cell surface display system has shortcomings. The molecular weight of the polypeptide or protein displayed on the phage cannot be too large; otherwise, it will affect the assembly and infection of the phage. Although the protein molecular mass displayed by the bacterial surface is improved, bacterial display lacks the process of post-translational modification of eukaryotic proteins.[35] Yeast display is prone to excessively high mannose glycosylation effects, and multisubunit proteins may be inactivated.[36] Although *B. subtilis* spore display has strong stress resistance,[37] the compatibility of protein expression needs to be further improved.[10] Therefore, it is highly valuable to construct an efficient and stable surface display system with strong universality and good stress resistance properties.

Baker's yeast, *Saccharomyces cerevisiae*, is generally recognized as a safe (GRAS) microorganism and is widely used in the food industry.[38] Although yeast surface display has been extensively studied, the construction of a surface display system based on yeast spores is rarely reported. Under starvation conditions, vegetative yeast cells (diploid) initiate the meiosis program and produce dormant cells termed spores (haploid).[39,40] Different from the vegetative yeast cell wall, which is composed of a β-glucan and mannan two-layer structure,[41] the spore wall of yeast contains a four-layer structure: mannan, glucan, chitosan, and dityrosine layers (from inside to outside). In particular, the outer two layers, chitosan and dityrosine, are unique structures of the spore wall, which is essential for the enhanced stress resistance properties of spores.[42,43] In addition to high safety, yeast spore surface display also has special advantages. First, proteins can be successfully displayed on the spore surface without the process of passing through the cell membrane, significantly improving the protein folding and

Received: March 21, 2022
Revised: May 24, 2022
Accepted: May 26, 2022
Published: June 9, 2022

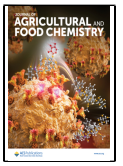

Table 1. Strains Used in This Study

strains	genotype	source
BL21(DE3)	F⁻ *Omp Thsd* $ThsdS_B$ (*rB-mB-*) *gal* dcm (DE3)	lab stock
S. cerevisiae AH109	*MATa trp1-901 leu2-3 112 ura3-52 his-200 gal4Δ gal80Δ LYS2::GAL1UAS-GAL1TATA-HIS3 MEL1 GAL2UAS-GAL2TATA-ADE2 URA3::MEL1UAS-MEL1TATA-lacZ*	lab stock
S. cerevisiae AN120 (wild-type)	*MATα/MATa ARG4/arg4-NspI his3ΔSK/his3ΔSK ho::LYS2/ho::LYS2 leu2/leu2 lys2/lys2 RME1/rme1::LEU2 trp1::hisG/ trp1::hisG ura3/ura3*	lab stock
S. cerevisiae AN262 (*chs3Δ*)	*MATα/MATa ARG4/arg4-NspI his3ΔSK/his3ΔSK ho::LYS2/ho::LYS2 leu2/leu2 lys2/lys2 RME1/rme1::LEU2 trp1::hisG/ trp1::hisG ura3/ura3 chs3Δ::his5+/ chs3Δ::his5+*	44
S. cerevisiae HW83 (*osw2Δ*)	*MATα/MATa ARG4/arg4-NspI his3ΔSK/his3ΔSK ho::LYS2/ho::LYS2 leu2/leu2 lys2/lys2 RME1/rme1::LEU2 trp1::hisG/ trp1::hisG ura3/ura3 osw2Δ::his5+/osw2Δ::his5+*	40
S. cerevisiae HW3 (*dit1Δ*)	*MATα/MATa ARG4/arg4-NspI his3ΔSK/his3ΔSK ho::LYS2/ho::LYS2 leu2/leu2 lys2/lys2 RME1/rme1::LEU2 trp1::hisG/ trp1::hisG ura3/ura3 dit1Δ::his5+/dit1Δ::his5+*	44

display efficiency. Second, proteins with high molecular weights or multisubunit structures can be efficiently displayed, avoiding possible inactivation using conventional surface display. Third, the unique stress resistance of yeast spores endows the tolerance of displayed proteins to multiple ambient pressures.

Interestingly, the spore wall of yeast is assembled *de novo* from inside to outside. For instance, the outermost layer of dityrosine is formed only after the assembly process of the second outermost layer of chitosan is completed. When the *DIT1* gene, which is required for dityrosine synthesis, is disrupted, the dityrosine layer cannot be formed, leading to chitosan layer exposure to the spore surface.[44] In our previous study, we established a nonhazardous biological approach for preparing natural "chitosan beads" based on *dit1Δ* mutant spores. Furthermore, the pure model enzymes *β*-galactosidase and D-psicose-3-epimerase were individually displayed on the surface of spore chitosan beads by activating the amino groups of chitosan using glutaraldehyde.[44,45] However, this method has disadvantages such as requiring the preparation of pure enzymes and the chemical agent glutaraldehyde for coupling. In this study, we developed a novel protein surface display system based on spore "chitosan beads". The target protein in fusion with the chitosan affinity protein (CAP) could be efficiently expressed and stably displayed on the surface of spores. Furthermore, the practicability of this surface display system was demonstrated for the semisynthesis of the paclitaxel intermediate.

MATERIALS AND METHODS

Strains and Plasmids Construction. The *Escherichia coli* DH5*α* strain was adopted for plasmid propagation and construction, and the *E. coli* BL21 (DE3) strain was used for protein expression. The genes for protein expression in BL21(DE3) were inserted into the pET28a plasmid and fused with a 6× His tag for protein purification. The gene *csn* encoding a chitosanase (CSN) was cloned from *B. subtilis* 168, and the mutant *csn* gene (csn^{E54Q}) was obtained by site-specific mutagenesis using the Fast Mutagenesis System (TransGen Biotech, Beijing, China). The *α*-galactosidase (*MEL1*) gene without the self-signal peptide sequence was cloned from *S. cerevisiae* AN109. The *β*-xylosidase gene from *Lentinula edodes* (*LXYL-P1-2*) was synthesized by BGI technology (Beijing, China), and the mutant *LXYL-P1-2* gene was obtained by site-specific mutagenesis. All *S. cerevisiae* strains used for sporulation in this research were in a fast-sporulating SK-1 background. To express the target protein on the surface of chitosan beads of *S. cerevisiae* spores, the signal peptide sequence (*ss*) of the Spr1 protein was fused with the *N*-terminus of the target protein and inserted into the pRS426 plasmid with a strong TEF1 promoter. All strains used in this study are summarized in Table 1 and were cultured as previously described.[40] The primers and recombinant plasmids are listed in Tables S1 and S2, respectively.

Overexpression and Purification of Related Enzymes in *E. coli*. The recombinant plasmid pET28a-csn^{E54Q} was transformed into *E. coli* BL21 (DE3) to overexpress the CAP protein. A single colony containing the pET28a-csn^{E54Q} plasmid was inoculated into 5 mL of LB medium with kanamycin (50 *μ*g/mL) at 37 °C overnight. Then, 1 mL of the seed culture was transferred to 100 mL of LB medium containing 50 *μ*g/mL kanamycin at 37 °C and 220 rpm. When the OD_{600} of the cell culture reached 0.6−0.8, isopropyl *β*-D-1-thiogalactopyranoside (IPTG) with a final concentration of 0.1 mM was added for CAP expression at 16 °C for 20 h. Next, the cells were collected by centrifugation at 9000 g for 5 min and resuspended in 50 mM Tris-HCl buffer (pH 7.5) for ultrasonication on ice. The supernatant of the crude enzyme was obtained by centrifugation at 12 000*g* for 30 min and loaded onto Ni^{2+}-NTA resin. The His-tagged CAP was eluted with 50 mM Tris-HCl buffer (pH 7.5) containing 500 mM imidazole. Finally, the purified enzyme was concentrated and desalted by an Amicon ultracentrifugal filter (10 kDa) using 50 mM Tris-HCl (pH 7.5). The purified CAP was preserved in 10% glycerol solution (v/v) at −20 °C for further use. The protein concentration was determined using a BCA Protein Assay Kit. The overexpression and purification of other recombinant proteins (CSN, GFP, or GFP-CAP) were carried out following a similar procedure as described above. The expression levels and purities of all related enzymes were detected by SDS-PAGE analysis. To detect the activity of CAP or CSN, the substrate chitosan was suspended in sodium acetate buffer (50 mM, pH 5.5) with a final concentration of 0.5% (wt/v). Then, the purified protein (CAP or CSN) was added at a final concentration of 0.2 mg/mL. The reaction was incubated at 50 °C for 20 min and stopped by boiling for 10 min.[46] The hydrolysate was qualitatively analyzed by thin-layer chromatography (TLC).[47]

Evaluation of the Binding Ability of CAP to the Surface of *dit1Δ* Spores. To evaluate the binding ability of CAP to the surface of *dit1Δ* spores *in vitro*, the pure fusion protein GFP-CAP with a final concentration of 0.1 mg/mL in 200 *μ*L of sodium acetate buffer (50 mM, pH 5.5) was mixed with 1 mg of purified *dit1Δ* spores and incubated at 25 °C and 800 rpm for 1 h. Then, the spores were washed using PBS three times (10 min each time). The fluorescence images for the localization of GFP-CAP protein were acquired using a laser confocal microscope model C2 with an excitation wavelength of 485 nm and an emission wavelength of 528 nm (Nikon, Tokyo, Japan). To quantify the fluorescence intensity of GFP located at the surface of *dit1Δ* spores using a microplate reader, the spores were resuspended in 200 *μ*L of sodium acetate buffer (50 mM, pH 5.5) and transferred to 96-well plates. To ensure reliability, the value of fluorescence intensity was normalized to the OD_{660} of spores. To evaluate the binding ability of CAP to the surface of *dit1Δ* spores *in vivo*, the recombinant plasmids pRS426-TEFpr-*ss-gfp-*csn^{E54Q}, pRS426-TEFpr-*ss-gfp-csn*, and pRS426-TEFpr-*ss-gfp* were transformed into the *S. cerevisiae dit1Δ* mutant strain. As a negative control, the plasmid pRS426-TEFpr-*ss-gfp-*csn^{E54Q} was also transformed into the *S. cerevisiae chs3Δ* mutant strain. The processes for the sporulation of the corresponding strains and isolation of spores were carried out as previously described.[40] For the binding stability assay, the corresponding spores after lyophilization (1 mg) were

https://doi.org/10.1021/acs.jafc.2c01983
J. Agric. Food Chem. 2022, 70, 7479−7489

washed three times using PBS containing 0.1% Triton X-100. The fluorescence images were observed using a laser confocal microscope as described below. The ascospores or purified spores were resuspended in PBS and the number of spores was kept ranging from 1.26×10^7 to 1.85×10^7. The samples were observed under a 100× oil-immersed confocal microscope. All microscopy images were obtained from three independently repeated experiments, and each group of images was guaranteed to be taken under the same fluorescence intensity and the same exposure time.

Western Blot Analysis. The purified spores (5−10 mg) were suspended in 300 μL of 8 M urea and treated with a freeze grinding machine for 20 min. The supernatant containing 100 μg protein obtained after centrifugation (4000*g*) was used for western blot analysis (5% concentrated gel and 10% separating gel). To analyze the glycosylation level of the protein, PNGase F was added to the supernatant to remove the glycan from the protein. The primary antibody was a mouse anti-HA/FLAG antibody (TransGen Biotech, Beijing, China) with a dilution ratio of 1:5000. The secondary antibody was horseradish peroxidase (HRP)-conjugated goat anti-mouse IgG (TransGen Biotech, Beijing, China) with a dilution ratio of 1:5000. The GAPDH antibody was used as an internal reference (Proteintech). The Clarity Western ECL substrate (Bio-Rad, Shanghai, China) was adopted to visualize the signals, and ImageQuant LAS4000 (GE Healthcare Bio-Science, Uppsala, Sweden) was applied to obtain the images.

α-Galactosidase (MEL1) Activity Assay. The activity of MEL1 was determined by measuring the generation of *p*-nitrophenol (*p*NP) using *p*-nitrophenyl-α-D-galactopyranoside (*p*NPG) as the substrate as described previously.[48] The standard reaction system was performed as follows: 2 mg of freeze-dried purified spores displaying MEL1 were suspended in 150 μL of citrate buffer (50 mM, pH 3.0) and preheated at 40 °C for 5 min. Then, 50 μL of *p*NPG (20 mM) was added and incubated at 40 °C for 10 min. To stop the reaction, 800 μL of sodium carbonate (250 mM) was added. Then, the supernatant was collected by centrifugation, and the amount of *p*NP released from *p*NPG was calculated by measuring the absorbance at 405 nm with a microplate reader. One enzyme unit (U) was defined as the amount of enzyme that produced 1.0 μmol of *p*NP from its substrate *p*NPG per minute. To detect the activity of free MEL1 in the culture supernatant, the supernatant was concentrated 100-fold with an Amicon-Ultra ultrafiltration tube (30 kDa). The effect of temperature on the activity of displayed MEL1 was examined using the standard reaction system described previously at different temperatures from 25 to 60 °C. The effect of pH on the activity of displayed MEL1 was investigated in 50 mM buffer from 1.0 to 10.0 (citrate buffer (pH 1.0−5.0); phosphate buffer (pH 6.0−7.0); Tris-HCl buffer (pH 8.0−10.0)). The reactions catalyzed by free MEL1 were used as a control. For the reusability assay, spores displaying MEL1 were recovered from the solution after each round of the reaction by centrifugation at 7000*g* for 5 min and extensively washed using 50 mM citrate buffer (pH 3.0) before the reaction was repeated.

β-Xylosidase (LXYL-P1−2) Activity Assay. The activity of LXYL-P1-2 was determined by measuring the amount of *p*NP produced from the substrate *p*-nitrophenyl-β-D-xylopyranoside (*p*NP-Xyl).[49] The reaction was carried out as follows: 2 mg of freeze-dried purified spores was suspended in 150 μL of sodium acetate buffer (50 mM, pH 4.5) and preheated at 50 °C for 5 min. Then, 50 μL of *p*NP-Xyl (20 mM) was added and incubated at 50 °C for 20 min. To stop the reaction, 800 μL of sodium carbonate (0.25 M) was added to the solution. The generation of *p*NP was monitored by measuring the absorbance at 405 nm using a microplate reader. One enzyme unit (U) was defined as the amount of enzyme that produced 1.0 nmol of *p*NP from *p*NP-Xyl at 50 °C, pH 4.5, per minute.

To detect the bioconversion of 7-β-xylosyl-10-deacetyltaxol (XDT) to 10-deacetyltaxol (DT) by surface-displayed LXYL-P1-2 for semisynthesis of paclitaxel, the standard reaction system (300 μL) was as follows: 50 mM sodium acetate buffer (pH 4.0) containing 0.5 mM XDT (dissolved in DMSO) and 6 mg of freeze-dried purified spores displaying LXYL-P1-2. The reaction was carried out at 45 °C overnight with shaking and terminated by adding ethyl acetate to extract the substrate and product.[50] The extracted solution was blown dry with nitrogen and reconstituted in anhydrous acetonitrile. The conversion rate of DT was analyzed by HPLC, and the detection conditions were as follows:[49] Waters Symmetry C18 column (4.6 mm × 250 mm, 5 μm), water-acetonitrile mobile phase (gradient, 0−12 min, acetonitrile volume 30−38%; 12−45 min, acetonitrile volume 38−52%), flow rate 1 mL/min, column temperature 26 °C, detection wavelength 230 nm.

Enzymatic Properties of LXYL-P1-2-CAP on the Spore Surface. To determine the effect of temperature on the activity of LXYL-P1-2-CAP displayed on the spore surface, the reaction was performed from 30 to 60 °C using 0.25 mM XDT as the substrate and free LXYL-P1-2 enzyme as a control. The effect of pH on the reactions was carried out in 50 mM buffers with pH values ranging from 3.0 to 6.5 (NaAc buffer (pH 3.0−5.5), sodium phosphate buffer (pH 6.0−6.5)) at 50 °C using free LXYL-P1-2 as a control. Next, the time courses for the conversion rates of DT were monitored by HPLC using different concentrations of XDT from 0.25 to 1 mM under optimized reaction conditions. Additionally, the reusability of displayed LXYL-P1-2-CAP or LXYL-P1-2 on the spore surface was evaluated in seven cycles of use. In each cycle, 20 g/L purified spores were mixed with 0.25 mM XDT in 50 mM sodium acetate buffer (pH 4.0) and incubated at 50 °C for 2 h. After the reaction was completed, the residual activity was measured. Before the next round of reaction was initiated, the spores were recovered by centrifugation and washed thoroughly with sodium acetate buffer (pH 4.0). The initial activity was defined as 100%, and the residual activity of each cycle was calculated according to the initial activity.

Stress Resistance of LXYL-P1-2-CAP Displayed on the Spore Surface. For the proteinase K tolerance assay, purified spores displaying LXYL-P1-2-CAP and free enzyme were resuspended in 50 mM Tris-HCl buffer (pH 7.5) containing 10 mM $CaCl_2$ and 8 U/mL proteinase K at 37 °C for 1 h. The activity of untreated spores or free enzyme was defined as 100%, and the residual activity was calculated according to the activity without treatment. For the long-term storage stability assay, the purified spores displaying LXYL-P1-2-CAP and free enzyme were placed in a dry environment at ambient temperature for eight and four weeks, respectively. The hydrolytic activities were measured every week using *p*NP-Xyl as the substrate. Additionally, the equivalent amount of spores or free enzyme stored at −20 °C was used as a control each time. For the organic reagent tolerance assay, the purified spores displaying LXYL-P1-2-CAP and free enzyme were resuspended in 75% (v/v) various organic reagents (acetonitrile, ethanol, ethyl acetate, ether, trichloromethane, toluene, cyclohexane, *n*-hexane or petroleum ether) and incubated at 25 °C for 24 h. Then, the residual activities were detected using XDT as the substrate as described above.

Cold Field Emission Scanning Electron Microscope (CFE-SEM) Imaging. To observe the surface of *dit1*Δ spores displaying LXYL-P1-2-CAP, freshly purified spores were suspended in water or purified spores after lyophilization were treated with 75% acetonitrile or anhydrous acetonitrile for 12 h at room temperature and then centrifuged. The samples were fixed with 5% glutaraldehyde at 4 °C overnight. Then, the fixed samples were rinsed several times with 0.1 M phosphate buffer. Next, the samples were dehydrated with different concentrations of ethanol (30, 50, 70, 90, and 100%), followed by critical point drying (CPD-300 LEICA company) and ion sputtering (ACE-600 LEICA company). Finally, the treated samples were observed by CFESEM (SU8220 HITACHI company).

RESULTS AND DISCUSSION

CAP Exhibited Strong Binding Capability with "Chitosan Beads" *In Vitro*. To develop an efficient surface display system based on these natural "chitosan beads" of yeast spores, seeking a chitosan affinity protein (CAP) that could efficiently bind to *dit1*Δ spores was one of the prerequisites. Chitosanases can interact with their substrate chitosan and degrade chitosan into chitooligosaccharide. Therefore, it was feasible that CAPs could be acquired by retaining chitosan

https://doi.org/10.1021/acs.jafc.2c01983
J. Agric. Food Chem. 2022, 70, 7479−7489

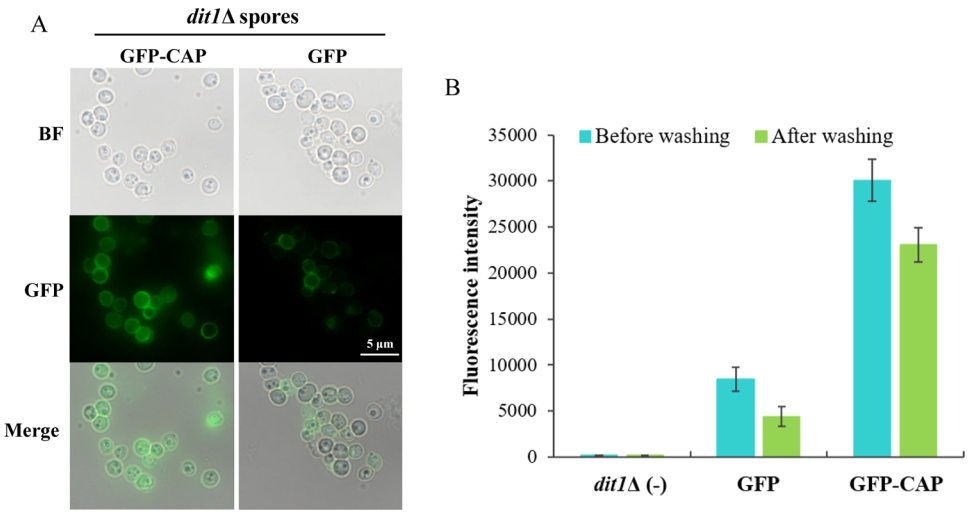

Figure 1. Evaluation of the binding ability of CAP with *dit1*Δ spores *in vitro*. (A) Binding strength of GFP-CAP/GFP with *dit1*Δ spores after washing *in vitro*. Spores were observed under a bright-field (BF) or laser confocal (GFP) microscope. Bar, 5 μm. (B) Comparison of the fluorescence intensity of *dit1*Δ spores incubated with GFP/GFP-CAP proteins before and after washing.

binding domains of chitosanases and mutating key amino acid residues located at catalytic domains.[51] Under this assumption, we focused on the chitosanase (CSN) from *B. subtilis* 168, and the catalytic glutamic acid residue at position 54 (information from UniProt database) was mutated to glutamine by site-directed mutagenesis. This chitosanase mutant CSN_{E54Q} was overexpressed in *E. coli* and obtained with high purity according to SDS-PAGE analysis (Figure S1A). Next, the hydrolytic activity of CSN_{E54Q} was evaluated by TLC analysis using chitosan as the substrate and a chitooligosaccharide mixture $(GlcN)_1$-$(GlcN)_6$ as a reference standard. As shown in Figure S1B, the hydrolytic activity of CSN_{E54Q} was significantly reduced, and the products were a small amount of $(GlcN)_3$ and oligosaccharides with a higher degree of polymerization. In contrast, the hydrolyzed products for wild-type CSN_{Bs} were a large amount of $(GlcN)_2$-$(GlcN)_3$ oligosaccharides. Therefore, the mutated enzyme CSN_{E54Q} was considered as a CAP. To evaluate the binding capability of CAP to *dit1*Δ spores *in vitro*, GFP was fused at the N-terminus of CAP, and the fusion protein GFP-CAP was expressed in *E. coli* and purified by nickel affinity chromatography (Figure S1C). Then, the purified GFP-CAP protein was incubated with *dit1*Δ spores, and confocal fluorescence microscopy illustrated that the fluorescence intensity of GFP-CAP bound to *dit1*Δ spores was much higher than that of GFP only (Figure 1A,B). Interestingly, the fluorescence intensity was not significantly decreased even after washing with PBS (Figure 1B). The possible explanation was that GFP fusion with CAP could strongly associate with the chitosan layer, and GFP without fusion with CAP showed weak binding capacity to the chitosan layer by weak electrostatic interactions. These results indicated that CAP played a decisive role and exhibited strong binding capability to "chitosan beads" *in vitro*.

CAP Showed Good Binding Capability with "Chitosan Beads" *In Vivo*. To evaluate the binding capability of CAP to "chitosan beads" of *dit1*Δ spores *in vivo*, CAP containing an *N*-terminal signal peptide was expressed in *dit1*Δ spores using wild-type CSN as a control. After confirming the expression of CAP and CSN by western blot analysis (Figure 2A), the localization of CAP was further investigated by fusion expression with GFP. As illustrated in Figure 2B, the green fluorescence of GFP-CAP protein could be observed around the surface of spore wall, while the fluorescence of GFP-CSN and free GFP was dispersed in the cytoplasm of the spore ascus. It was worth noting that a certain amount of GFP-CAP protein was located in the center of spores, although the reason for this orientation was unclear. To prove that the binding capability of CAP was dependent on the chitosan layer of the *dit1*Δ spore wall, the fusion protein GFP-CAP was expressed in *chs3*Δ spores. Different from *dit1*Δ spores, the spore wall of *chs3*Δ spores has two layers, and the outermost layer is the *β*-glucan layer.[44] As shown in Figure 2B, the fluorescence of GFP-CAP in *chs3*Δ spores was also dispersed in the cytoplasm of the ascus, which confirmed our hypothesis. To assay the binding stability of CAP toward the chitosan layer of the spore wall, the ascus of *dit1*Δ spores was disrupted, and the released spores were further purified and washed with PBS. As shown in Figure 2C, the fluorescence of GFP-CAP protein in *dit1*Δ spores was almost completely retained on the spore wall after washing, while the fluorescence from the control groups was nearly completely washed off. These results demonstrated that CAP exhibited good binding capability with the *dit1*Δ spore *in vivo* and could be used in the surface display system in the following study.

Verification of the Established Surface Display Platform Based on "Chitosan Beads". To verify the performance of this surface display system, the secreted form MEL1 fused with the *N*-terminus of CAP was used as a model enzyme. According to western blot analysis, the control protein MEL1 and the fusion protein MEL1-CAP were both expressed in "chitosan beads" of *dit1*Δ spores. However, the protein molecular weights were higher than the theoretical values (Figure 3A), indicating that MEL1 was glycosylated. As we expected, the molecular weights of MEL1 protein were decreased to the theoretical values after the removal of the *N*-glycan by PNGase F (Figure 3B). Next, the enzyme activity of MEL1-CAP displayed on the surface of the *dit1*Δ spore was examined. As shown in Figure 3C, the activity of MEL1-CAP in *dit1*Δ spores was approximately 3.17 times higher than that of MEL1 without CAP. To clarify the reason, the enzyme activity in the sporulation medium (supernatant of KAc medium) was also tested, and the total enzyme activity was

https://doi.org/10.1021/acs.jafc.2c01983
J. Agric. Food Chem. 2022, 70, 7479−7489

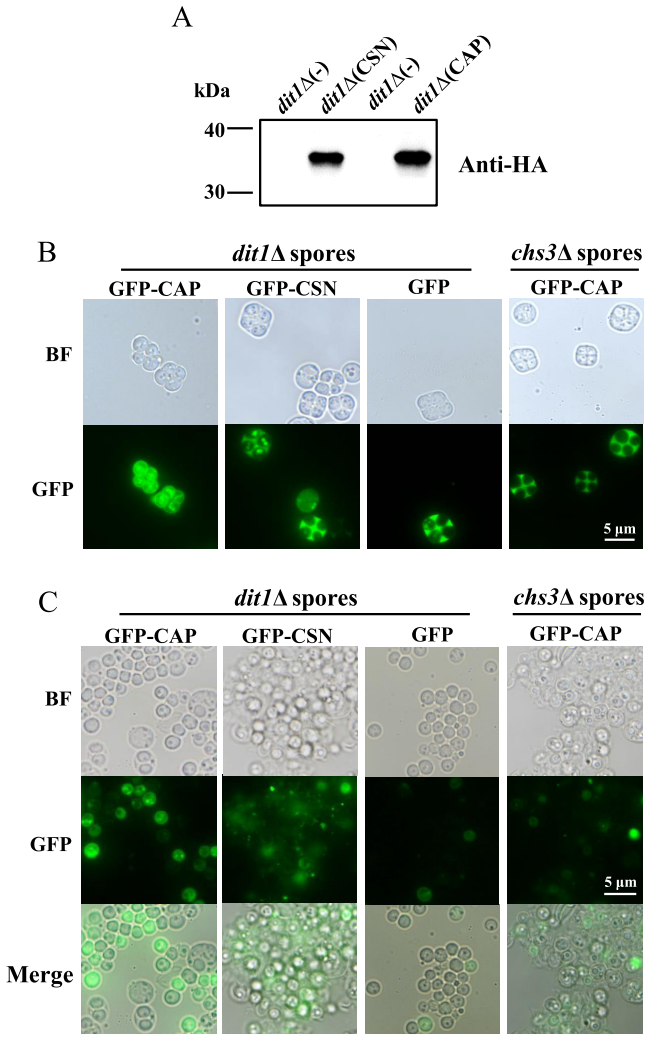

Figure 2. Evaluation of the binding ability of CAP with *dit1*Δ spores *in vivo*. (A) Western blot detection of CAP (34 kDa) expression in *dit1*Δ spores. *dit1*Δ(−) harboring the empty plasmid, *dit1*Δ(CSN) and *dit1*Δ(CAP) representing *dit1*Δ spores expressing CSN and CAP, respectively. (B) Localization of GFP-CAP in *dit1*Δ spores. (C) Binding ability of GFP-CAP with *dit1*Δ spores after washing *in vivo*. Spores were observed under a bright-field (BF) or laser confocal (GFP) microscope. Bar, 5 μm.

calculated. As shown in Figure 3D the activity of MEL1 without CAP in the KAc medium was approximately 3 times higher than that of MEL1-CAP, but the total enzyme activities for MEL1-CAP and MEL1 were almost equivalent. The explanation for this phenomenon was that MEL1 in fusion with CAP was tightly bound to the chitosan layer, which significantly increased the activity of the enzyme displayed on the surface of "chitosan beads". Simultaneously, the leakage of the MEL1-CAP fusion protein into the sporulation medium was greatly decreased.

Next, the enzymatic properties of MEL1-CAP displayed on the spore surface were evaluated using free MEL1 as a control. The optimum temperatures of displayed MEL1-CAP and free MEL1 were both 40 °C. When the temperature was higher than 40 °C, the displayed enzyme showed higher activity (Figure S2A). In addition, the displayed and free enzymes both exhibited the highest activity at pH 3.0. In contrast to free MEL1, MEL1-CAP displayed on the spore surface could tolerate a broader range of pH values and efficiently catalyze the reaction from pH 2.0−4.0 (Figure S2B). Furthermore, the reusability of the displayed MEL1-CAP was evaluated using the displayed MEL1 without CAP fusion as a control. As shown in Figure S2C, MEL1 in fusion with CAP exhibited good reusability, and 75% of the initial activity was maintained after five rounds of reuse. In contrast, the reusability of MEL1 was unsatisfactory, and less than 50% of the initial activity was retained after an equal number of reuses. Together, these results suggested that CAP could be used as a potential scaffold protein to efficiently display various proteins on the surface of "chitosan beads".

Surface Display of LXYL-P1-2-CAP Using "Chitosan Beads" and Its Potential Application in Paclitaxel Intermediate Production. To demonstrate the practicability of this surface display system, a β-xylosidase named LXYL-P1-2, which is involved in the key reaction step for the production of paclitaxel, was selected. LXYL-P1-2 catalyzes the conversion of 7-β-xylosyl-10-deacetyltaxol (XDT) to 10-deacetyltaxol (DT) by releasing the D-xylosyl group at the C-7 position, and DT can be further converted to paclitaxel by an acetyltransferase.[52] As a tetrameric macromolecular protein,[53] LXYL-P1-2 has 10 glycosylation sites, and the molecular weight is approximately 110 kDa after glycosylation (Figure 4A). To date, the cell surface display of LXYL-P1-2 in microorganisms has not been achieved because of its high molecular weight and complicated structure. Different from traditional cell surface display systems, proteins are not required to be transported across the membrane for the surface display platform using yeast spores, which is advantageous for displaying complex proteins in their active form. LXYL-P1-2 was first expressed in three different types of spores (*dit1*Δ, *osw2*Δ, and wild-type AN120), and the results showed that *dit1*Δ spores had the highest activity (Figure S3), which was consistent with our previous study.[43]

Then, LXYL-P1-2 was fused with CAP at the N-terminus to replace MEL1 as described above. The expression of LXYL-P1-2-CAP in "chitosan beads" was examined by Western blot assay. As shown in Figure 4A, the expression level of LXYL-P1-2-CAP was much higher than that of LXYL-P1-2 without CAP, which could be explained by the fact that more protein was bound to the spore wall due to the interaction of CAP with the chitosan layer. To verify that LXYL-P1-2-CAP was displayed on the spore surface, freshly purified spores were observed by CFESEM. Compared with the *dit1*Δ spores expressing the empty vector, the *dit1*Δ spores displaying LXYL-P1-2-CAP on the surface were larger and had a rougher surface (Figure 4B), indicating that the target proteins were enriched on the spore surface.

Next, the activity and conversion rate of spores displaying LXYL-P1-2 were detected. As shown in Figure 4C,D, the activity and conversion rate of LXYL-P1-2-CAP were 1.67 times and 1.65 times higher than those of LXYL-P1-2, respectively, which was attributed to the increased amount of protein bound to the spore wall. A previous study showed that the activity of the LXYL-P1-2 mutant (S449A) was obviously improved in *Pichia pastoris*.[53] Inspired by this result, an LXYL-P1-2 mutant (S449A) was constructed and displayed on the surface of *dit1*Δ spores. Compared with LXYL-P1-2-CAP, the activity of LXYL-P1-2(S449A)-CAP was increased by 1.71-fold against *p*NP-Xyl (Figure 4C), and the conversion rate of this mutant was also improved from 55 to 81% against XDT (Figure 4D). Therefore, "chitosan beads" displaying LXYL-P1-2(S449A)-CAP were used in the following study. Moreover,

https://doi.org/10.1021/acs.jafc.2c01983
J. Agric. Food Chem. 2022, 70, 7479−7489

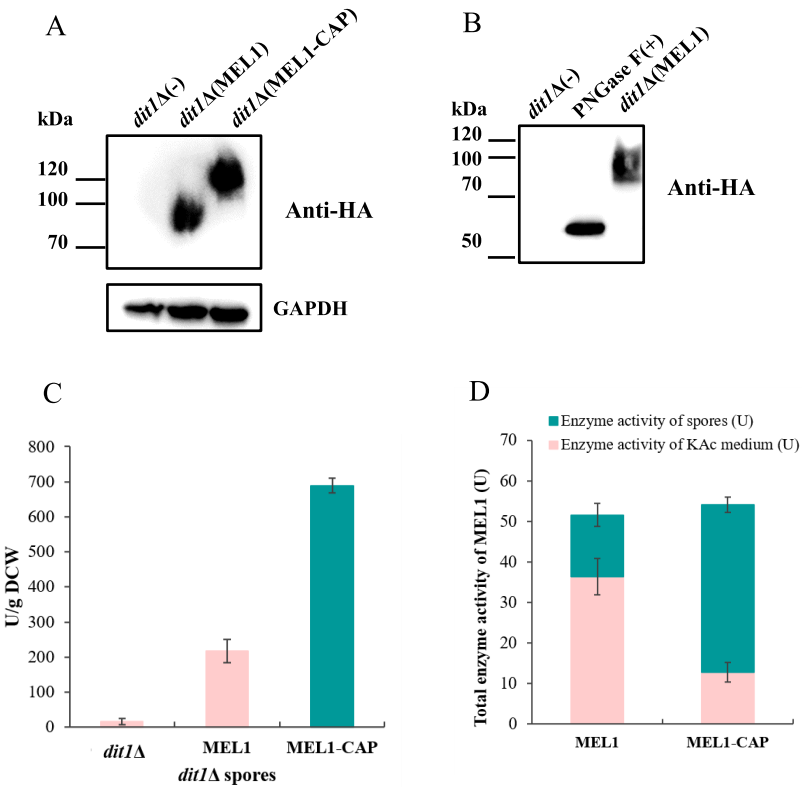

Figure 3. MEL1 was used as a model enzyme to verify the performance of the surface display system. (A) Western blot detection of MEL1 (57 kDa) and MEL1-CAP (82 kDa) expression in *dit1*Δ spores using GAPDH as an internal reference. (B) Western blot detection of MEL1 treated with the PNGase F enzyme. (C) Activity of MEL1 and MEL1-CAP displayed on the surface of *dit1*Δ spores. (D) Total enzyme activity in the spores and medium during sporulation.

the reaction product DT catalyzed by spore surface-displayed LXYL-P1-2 was confirmed by HPLC and MS (Figure S4A,B).

LXYL-P1-2-CAP Displayed on the Spore Surface Exhibited Preferred Enzymatic Properties. Immobilized enzymes with improved enzymatic properties are highly valued in industries and have become a benchmark for evaluating the performance of biocatalysts.[54] As shown in Figure 5A, the optimum temperature of LXYL-P1-2-CAP displayed on the spore surface was 50 °C, which was quite similar to that of free enzyme. However, the spore displaying LXYL-P1-2-CAP showed higher activities at elevated temperatures, indicating an increased thermostability of spore-displaying enzyme. The possible reason was that the covalent bond formation between the enzyme and chitosan layer was capable of increasing the conformational rigidity of the enzyme and the activation energy of the thermal denaturation reaction.[55] The pH is another key factor for enzymes to maintain their catalytic activity because the ionic charge of amino acids may influence the enzymatic conformation.[56,57] For the spore surface displaying LXYL-P1-2-CAP, the optimum pH was 4.0, which is more acidic than the optimum pH of 4.5 of the free enzyme (Figure 5B). The displayed LXYL-P1-2-CAP showed better acid resistance since its relative activities at pH 3.0 and 3.5 were maintained at nearly 40% and 100% of the highest activity, respectively, whereas the free enzyme maintained only 9 and 52% of the highest activity at the same pH values. For the time courses of DT synthesis, the conversion rate at equilibrium decreased gradually with increasing substrate concentration, and the highest conversion rate was 92% using 0.25 mM XDT (Figure 5C). For the reusability assay, the activity of spores displaying LXYL-P1-2-CAP retained more than 60% of the initial activity after seven cycles of reuse, while the activity of LXYL-P1-2 without CAP was less than 20% of the initial activity under the same processing conditions (Figure 5D). These results proved that the scaffold protein CAP not only increased the amounts of enzymes bound to the spore surface but also effectively improved the reusability of enzymes displayed on the spore surface.

LXYL-P1-2-CAP Displayed on the Spore Surface Exhibited Higher Resistance to Environmental Stresses. Proteinase K is a powerful proteolytic enzyme that can strongly digest proteins, including enzymes. First, the resistance of the spore wall to proteinase K was evaluated. As shown in Figure 6A, the activity of free LXYL-P1-2 was reduced to 35% of the initial activity after the treatment. It is worth noting that spores displaying LXYL-P1-2-CAP still exhibited 70% residual activity. This finding proved that the chitosan layer alone could also resist degradation by proteinase K toward the displaying enzyme to a certain extent. Storage stability is one of the main factors limiting the industrial application of immobilized enzymes. As shown in Figure S5, the residual activity of LXYL-P1-2-CAP displayed on the spore surface was still maintained at approximately 75% after 8 weeks. In contrast, the activity of free LXYL-P1-2 remained at less than 40% after 4 weeks.

In addition, the tolerance of LXYL-P1-2-CAP displayed on the spore surface to various organic reagents was verified using free LXYL-P1-2 as a control (Figure 6B). The relative activity of spores displaying LXYL-P1-2-CAP treated with NaAc buffer (pH 4.0) was set to 100%. As shown in Figure 6B, the spore displaying LXYL-P1-2-CAP was capable of resisting various organic solutions with a concentration up to 75% (v/v), and

https://doi.org/10.1021/acs.jafc.2c01983
J. Agric. Food Chem. 2022, 70, 7479−7489

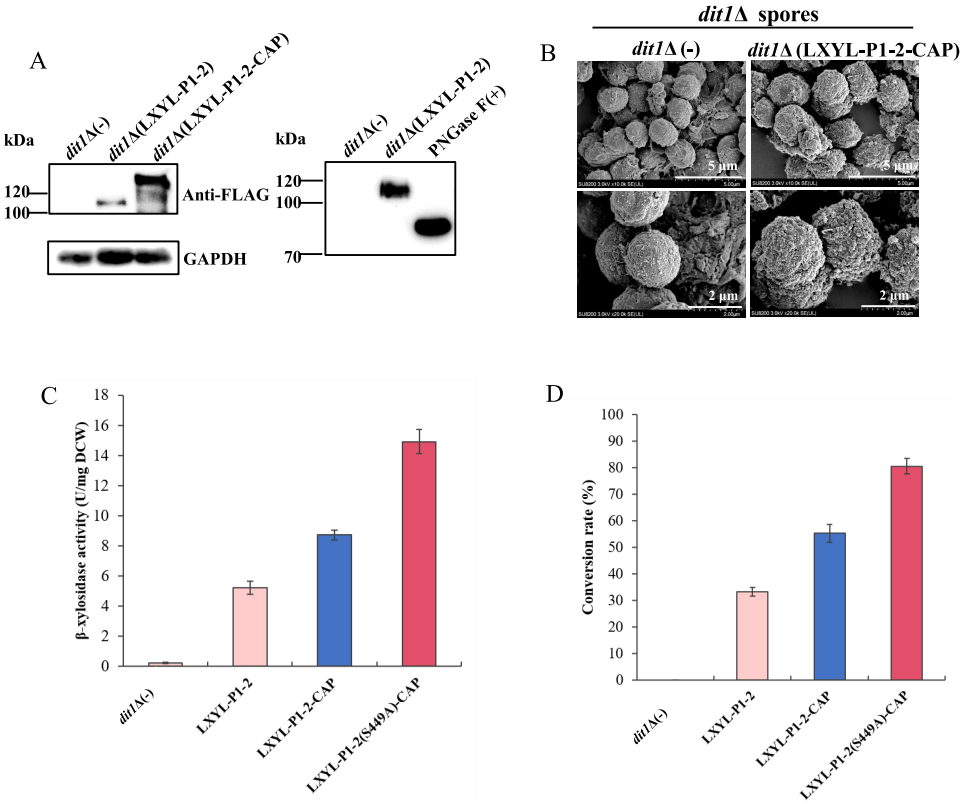

Figure 4. Application of LXYL-P1-2 in the yeast spore surface display system. (A) Western blot analysis of LXYL-P1-2 (92 kDa) and LXYL-P1-2-CAP (123 kDa) expression in *dit1*Δ spores using GAPDH as an internal reference. LXYL-P1-2 was treated with the PNGase F enzyme on the right side. *dit1*Δ(−) harboring the empty plasmid, *dit1*Δ(LXYL-P1-2), and *dit1*Δ(LXYL-P1-2-CAP) representing *dit1*Δ spores expressing LXYL-P1-2 and LXYL-P1-2-CAP, respectively. (B) CFESEM images of *dit1*Δ spores without (left) or with (right) LXYL-P1-2-CAP displayed on the spore surface. Bar, 5 μm (above), 2 μm (below). (C) Activity of displayed LXYL-P1-2-CAP against 5 mM *p*NP-Xyl. (D) Conversion rate for the displayed LXYL-P1-2 against 0.5 mM XDT.

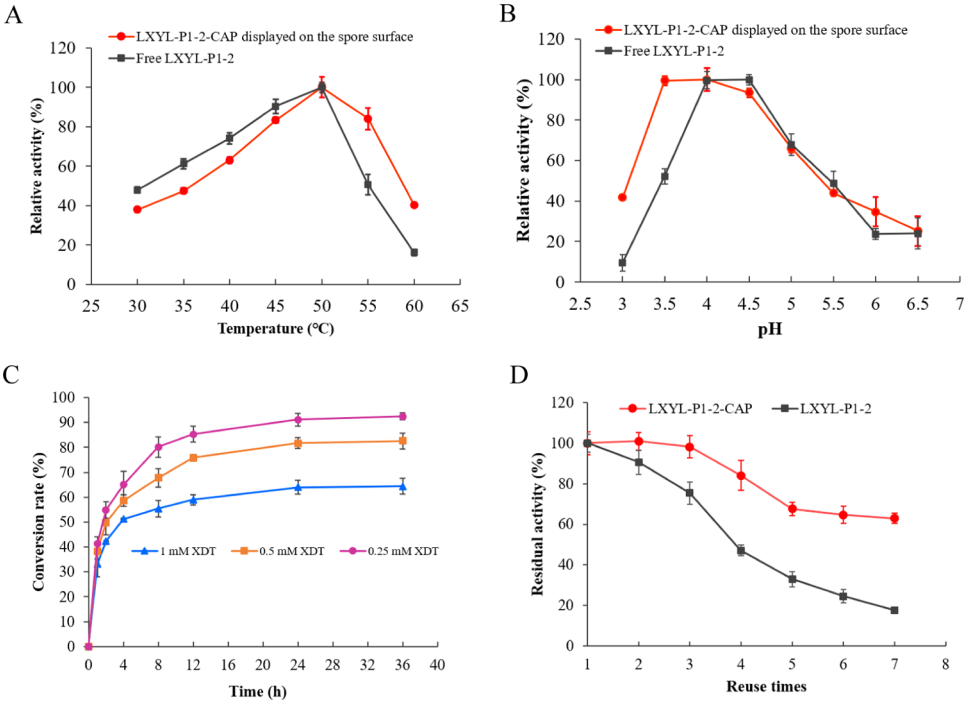

Figure 5. Enzymatic properties of LXYL-P1-2-CAP displayed on the spore surface against XDT. Effect of temperature (A) and pH (B) on the activity of displayed LXYL-P1-2-CAP using free LXYL-P1-2 as a control. (C) Time courses of DT production from XDT at different concentrations under optimal conditions. (D) Reusability of displayed LXYL-P1-2 with or without CAP.

https://doi.org/10.1021/acs.jafc.2c01983
J. Agric. Food Chem. 2022, 70, 7479−7489

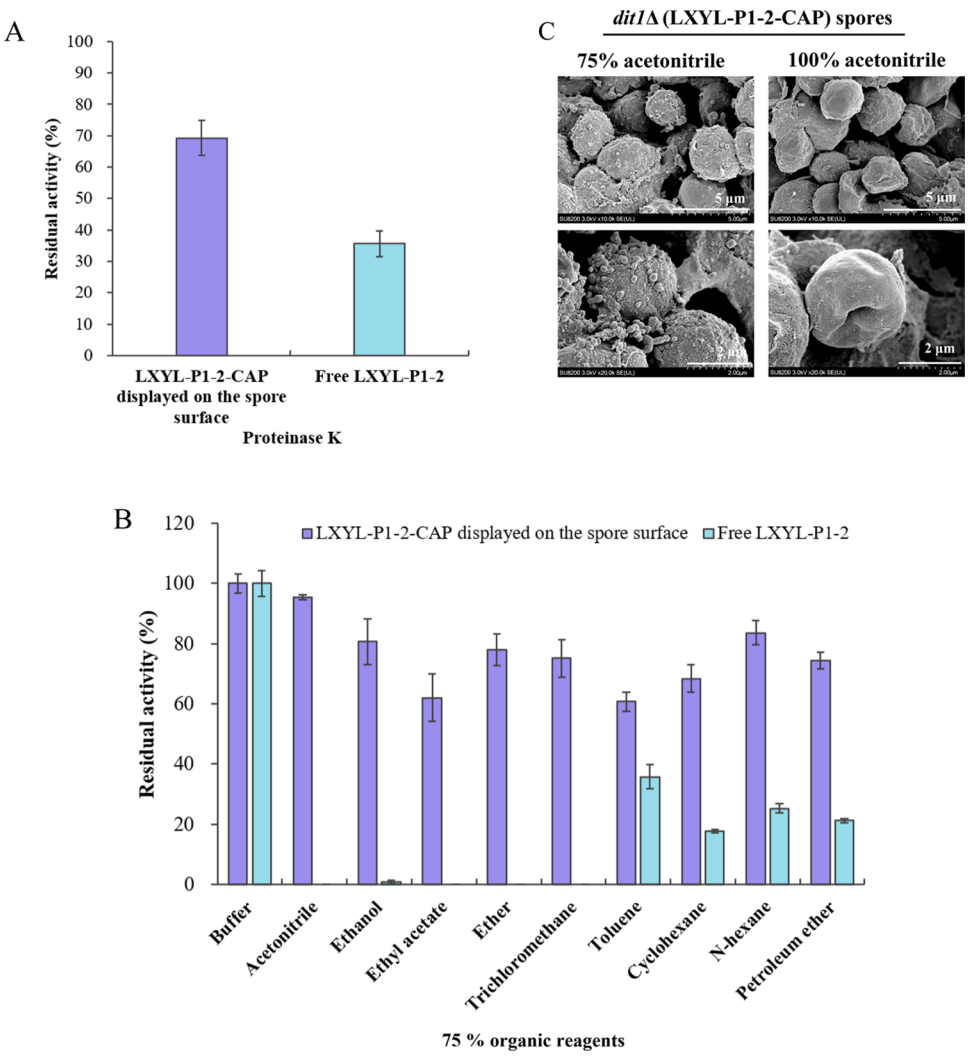

Figure 6. Resistance of LXYL-P1-2-CAP displayed on the spore surface toward diverse environmental stresses compared with free LXYL-P1-2. (A) Tolerances of displayed LXYL-P1-2-CAP toward proteinase K. (B) Tolerances of displayed LXYL-P1-2-CAP toward 75% organic reagents. (C) CFESEM images of the surface of lyophilized purified spores displaying LXYL-P1-2-CAP treated with 75% acetonitrile (left) or anhydrous acetonitrile (right).

the relative activities were all maintained above 60% of the highest activity. In contrast, the relative activity of free LXYL-P1-2 was significantly decreased, and the activity was retained below 40%. It is worth noting that the free enzyme almost lost its activity in acetonitrile, ethanol, ethyl acetate, ether, or trichloromethane, while the spore displaying LXYL-P1-2-CAP maintained more than 60% relative activity under the same conditions. To further explore the resistance mechanism to organic reagents, acetonitrile was selected because the tolerance of spore-displaying enzymes to this reagent was the highest. When the purified spores were lyophilized and treated with anhydrous acetonitrile (100%), the surface of the spores was shrunken according to the CFESEM results (Figure 6C). In contrast, after treatment with 75% acetonitrile, the lyophilized spores began to swell due to the absorption of water, and the shape of the spores became spherical. Therefore, we suspected that in the presence of 75% acetonitrile, a film of water was formed at the surface of spore "chitosan beads", which provided an aqueous environment for the displayed enzymes and protected the enzyme from organic reagents.

In summary, a novel and useful protein surface display system based on "chitosan beads" of yeast spores was established. Quite different from the display system using *B. subtilis* spores, which uses capsid proteins of the spore wall as anchor proteins, a chitosan affinity protein was identified and adopted as a scaffold to efficiently and stably display the target protein on the chitosan layer of yeast spores in this study. Our method avoids displaying proteins embedded in the membrane or folded intracellularly and allows more proteins to be displayed on the spore surface. To our delight, this surface display system showed high stress resistance, reusability, and excellent tolerance to organic reagents. The practicability of this surface display system was also verified for the semisynthesis of paclitaxel intermediate DT. Based on the well-proven utility of this system, this approach can be easily extended to the immobilization of other enzymes, especially for multimeric macromolecular proteins of eukaryotic origin. Compared with most nanomaterials for enzyme immobilization requiring the preparation of pure enzyme, the natural "chitosan beads" of yeast spores serve as a potential engineering living material (ELM), which can achieve protein expression and immobilization during the sporulation process. We believe that this surface display platform will have a wide range of applications,

https://doi.org/10.1021/acs.jafc.2c01983
J. Agric. Food Chem. 2022, 70, 7479−7489

benefiting the fields of biocatalysis, environmental protection, and the food and pharmaceutical industries.

■ ASSOCIATED CONTENT

Supporting Information

The Supporting Information is available free of charge at https://pubs.acs.org/doi/10.1021/acs.jafc.2c01983.

Primers (Table S1); plasmids (Table S2), and experimental results (Figures S1−S5) (PDF)

■ AUTHOR INFORMATION

Corresponding Authors

Zijie Li − *Key Laboratory of Carbohydrate Chemistry and Biotechnology, Ministry of Education, School of Biotechnology, Jiangnan University, Wuxi 214122 Jiangsu, China;* orcid.org/0000-0002-5618-1862; Email: lizijie@jiangnan.edu.cn

Xiao-Dong Gao − *Key Laboratory of Carbohydrate Chemistry and Biotechnology, Ministry of Education, School of Biotechnology, Jiangnan University, Wuxi 214122 Jiangsu, China;* orcid.org/0000-0002-8575-5095; Email: xdgao@jiangnan.edu.cn

Authors

Wanjie Li − *Key Laboratory of Carbohydrate Chemistry and Biotechnology, Ministry of Education, School of Biotechnology, Jiangnan University, Wuxi 214122 Jiangsu, China*

Yasen Wang − *Key Laboratory of Carbohydrate Chemistry and Biotechnology, Ministry of Education, School of Biotechnology, Jiangnan University, Wuxi 214122 Jiangsu, China*

Zhou Chen − *Key Laboratory of Carbohydrate Chemistry and Biotechnology, Ministry of Education, School of Biotechnology, Jiangnan University, Wuxi 214122 Jiangsu, China*

Hideki Nakanishi − *Key Laboratory of Carbohydrate Chemistry and Biotechnology, Ministry of Education, School of Biotechnology, Jiangnan University, Wuxi 214122 Jiangsu, China*

Xiangyang Xu − *Zaozhuang Jienuo Enzyme Co., Ltd., Zaozhuang 277100, China*

Complete contact information is available at: https://pubs.acs.org/10.1021/acs.jafc.2c01983

Author Contributions

[§]Z.L. and W.L. contributed equally to this work.

Notes

The authors declare no competing financial interest.

■ ACKNOWLEDGMENTS

This work was supported by National Natural Science Foundation of China (no. 32171475, 31971216), Shandong Provincial Major Scientific and Technological Innovation Project (no. 2019JZZY011006), Natural Science Foundation of Jiangsu Province (no. BK20210465), and Postgraduate Research&Practice Innovation Program of Jiangsu Province (SJCX20_0743).

■ REFERENCES

(1) Pham, M. L.; Polakovic, M. Microbial cell surface display of oxidoreductases: Concepts and applications. *Int. J. Biol. Macromol.* **2020**, *165*, 835−841.

(2) McMahon, C.; Baier, A. S.; Pascolutti, R.; Wegrecki, M.; Zheng, S. D.; Ong, J. X.; Erlandson, S. C.; Hilger, D.; Rasmussen, S. G. F.; Ring, A. M.; Manglik, A.; Kruse, A. C. Yeast surface display platform for rapid discovery of conformationally selective nanobodies. *Nat. Struct. Mol. Biol.* **2018**, *25*, 289.

(3) Salema, V.; Fernandez, L. A. *Escherichia coli* surface display for the selection of nanobodies. *Microb. Biotechnol.* **2017**, *10*, 1468−1484.

(4) Zhang, H. Y.; Chu, W. Q.; Sun, J. N.; Liu, Z.; Huang, W. C.; Xue, C. H.; Mao, X. Z. Combining cell surface display and DNA-shuffling technology for directed evolution of *Streptomyces* phospholipase D and synthesis of phosphatidylserine. *J. Agric. Food Chem.* **2019**, *67*, 13119−13126.

(5) Guirimand, G.; Inokuma, K.; Bamba, T.; Matsuda, M.; Morita, K.; Sasaki, K.; Ogino, C.; Berrin, J. G.; Hasunuma, T.; Kondo, A. Cell-surface display technology and metabolic engineering of *Saccharomyces cerevisiae* for enhancing xylitol production from woody biomass. *Green Chem.* **2019**, *21*, 1795−1808.

(6) Fan, S.; Liang, B.; Xiao, X. X.; Bai, L.; Tang, X. J.; Lojou, E.; Cosnier, S.; Liu, A. H. Controllable display of sequential enzymes on yeast surface with enhanced biocatalytic activity toward efficient enzymatic biofuel cells. *J. Am. Chem. Soc.* **2020**, *142*, 3222−3230.

(7) Park, M. Surface display technology for biosensor applications: A Review. *Sensors* **2020**, *20*, No. 2775.

(8) Liang, B.; Wang, G.; Yan, L.; Ren, H.; Feng, R. R.; Xiong, Z.; Liu, A. H. Functional cell surface displaying of acetylcholinesterase for spectrophotometric sensing organophosphate pesticide. *Sens. Actuators, B* **2019**, *279*, 483−489.

(9) Yao, Y. Y.; Yang, Y. L.; Gao, C. C.; Zhang, F. L.; Xia, R.; Li, D.; Hu, J.; Ran, C.; Zhang, Z.; Liu-Clarke, J.; Zhou, Z. G. Surface display system for probiotics and its application in aquaculture. *Rev. Aquacult.* **2020**, *12*, 2333−2350.

(10) Hsieh, H. Y.; Lin, C. H.; Hsu, S. Y.; Stewart, G. C. A *Bacillus* spore-based display system for bioremediation of atrazine. *Appl. Environ. Microb.* **2020**, *86*, No. e01230-20.

(11) Zhu, B. T.; Wei, N. Biocatalytic degradation of parabens mediated by cell surface displayed cutinase. *Environ. Sci. Technol.* **2019**, *53*, 354−364.

(12) Ding, J. M.; Liu, Y.; Gao, Y. X.; Zhang, C. B.; Wang, Y. F.; Xu, B.; Yang, Y. J.; Wu, Q.; Huang, Z. X. Biodegradation of λ-cyhalothrin through cell surface display of bacterial carboxylesterase. *Chemosphere* **2021**, *289*, No. 133130.

(13) Li, Z. D.; Yeh, M. Construction and diversity analysis of a murine IgE phage surface display library. *Cell Res.* **1997**, *7*, 161−170.

(14) Braun, R.; Schonberger, N.; Vinke, S.; Lederer, F.; Kalinowski, J.; Pollmann, K. Application of next generation sequencing (NGS) in phage displayed peptide selection to support the identification of arsenic-binding motifs. *Viruses* **2020**, *12*, No. 1360.

(15) Ren, S.; Fengyu; Zuo, S.; Zhao, M.; Wang, X.; Chen, Y.; Wu, Z.; Ren, Z.; Wang, X. Inhibition of tumor angiogenesis in lung cancer by T4 phage surface displaying mVEGFR2 vaccine. *Vaccine* **2011**, *29*, 5802−5811.

(16) Gallus, S.; Peschke, T.; Paulsen, M.; Burgahn, T.; Niemeyer, C. M.; Rabe, K. S. Surface display of complex enzymes by *in situ* SpyCatcher-SpyTag interaction. *ChemBioChem.* **2020**, *21*, 2126−2131.

(17) Palei, S.; Becher, K. S.; Nienberg, C.; Jose, J.; Mootz, H. D. Bacterial cell-surface display of semisynthetic cyclic peptides. *ChemBioChem.* **2019**, *20*, 72−77.

(18) Chen, Y.; Ling, Z.; Mamtimin, T.; Khan, A.; Peng, L.; Yang, J.; Ali, G.; Zhou, T.; Zhang, Q.; Zhang, J.; Li, X. Chitooligosaccharides production from shrimp chaff in chitosanase cell surface display system. *Carbohydr. Polym.* **2022**, *277*, No. 118894.

(19) Chen, Z. Z.; Wang, Y. Y.; Cheng, Y. Y.; Wang, X.; Tong, S. W.; Yang, H. T.; Wang, Z. F. Efficient biodegradation of highly crystallized

polyethylene terephthalate through cell surface display of bacterial PETase. *Sci. Total Environ.* **2020**, *709*, No. 136138.
(20) Gercke, D.; Furtmann, C.; Tozakidis, I. E. P.; Jose, J. Highly crystalline post-consumer PET waste hydrolysis by surface displayed PETase using a bacterial whole-cell biocatalyst. *ChemCatChem.* **2021**, *13*, 3479−3489.
(21) Dvořák, P.; Bayer, E. A.; de Lorenzo, V. Surface display of designer protein scaffolds on genome-reduced strains of *Pseudomonas putida*. *ACS Synth. Biol.* **2020**, *9*, 2749−2764.
(22) Nicolay, T.; Vanderleyden, J.; Spaepen, S. Autotransporter-based cell surface display in Gram-negative bacteria. *Crit. Rev. Microbiol.* **2015**, *41*, 109−123.
(23) Jeong, M. Y.; Rutter, J.; Chou, D. H. C. Display of single-chain insulin-like peptides on a yeast surface. *Biochemistry* **2019**, *58*, 182−188.
(24) Kajiwara, K.; Aoki, W.; Koike, N.; Ueda, M. Development of a yeast cell surface display method using the SpyTag/SpyCatcher system. *Sci. Rep.* **2021**, *11*, No. 11059.
(25) Liu, C.; Zhang, W.; Li, Y.; Pan, K.; OuYang, K.; Song, X.; Xiong, X.; Zang, Y.; Wang, L.; Qu, M.; Zhao, X. Characterization of yeast cell surface displayed *Lentinula edodes* xylanase and its effects on the hydrolysis of wheat. *Int. J. Biol. Macromol.* **2022**, *199*, 341−347.
(26) Gao, M. J.; Zhou, Y. C.; Yan, J. J.; Zhu, L.; Li, Z. T.; Hu, X. Y.; Zhan, X. B. Efficient precious metal Rh(III) adsorption by waste *P. pastoris* and *P. pastoris* surface display from high-density culture. *J. Hazard. Mater.* **2022**, *427*, No. 128140.
(27) Luo, B. B.; Jin, M. M.; Li, X. H.; Makunga, N. P.; Hu, X. B. Yeast surface display for *in vitro* biosynthetic pathway reconstruction. *ACS Synth. Biol.* **2021**, *10*, 2938−2946.
(28) Chun, J.; Bai, J.; Ryu, S. Yeast surface display system for facilitated production and application of phage endolysin. *ACS Synth. Biol.* **2020**, *9*, 508−516.
(29) Yang, K. X.; Li, F.; Qiao, Y. G.; Zhou, Q. H.; Hu, Z. M.; He, Y. J.; Yan, Y. J.; Xu, L.; Madzak, C.; Yan, J. Y. Design of a new multienzym ecomplex synthesis system based on *Yarrowia lipolytica* simultaneously secreted and surface displayed fusion proteins for sustainable production of fatty acid-derived hydrocarbons. *ACS Sustainable Chem. Eng.* **2018**, *6*, 17035−17043.
(30) Isticato, R.; Cangiano, G.; Tran, H. T.; Ciabattini, A.; Medaglini, D.; Oggioni, M. R.; De Felice, M.; Pozzi, G.; Ricca, E. Surface display of recombinant proteins on *Bacillus subtilis* spores. *J. Bacteriol.* **2001**, *183*, 6294−6301.
(31) Lin, P.; Yuan, H. B.; Du, J. K.; Liu, K. Q.; Liu, H. L.; Wang, T. F. Progress in research and application development of surface display technology using *Bacillus subtilis* spores. *Appl. Microbiol. Biotechnol.* **2020**, *104*, 2319−2331.
(32) Karava, M.; Gockel, P.; Kabisch, J. *Bacillus subtilis* spore surface display of photodecarboxylase for the transformation of lipids to hydrocarbons. *Sustainable Energy Fuels* **2021**, *5*, 1727−1733.
(33) Liu, H. L.; Yang, S. J.; Wang, X. H.; Wang, T. F. Production of trehalose with trehalose synthase expressed and displayed on the surface of *Bacillus subtilis* spores. *Microb. Cell Fact.* **2019**, *18*, No. 100.
(34) Mai, W.; Xin, J.; Yan, B. Oral immunizations with *Bacillus subtilis* spores expressing MCP protein provide protection against red-spotted grouper nervous necrosis virus (RGNNV) infection in juvenile grouper, Epinephelus coioides. *Aquacult. Int.* **2022**, *552*, No. 738008.
(35) Wan, H. M.; Chang, B. Y.; Lin, S. C. Anchorage of cyclodextrin glucanotransferase on the outer membrane of *Escherichia coli*. *Biotechnol. Bioeng.* **2002**, *79*, 457−464.
(36) Lozančić, M.; Hossain, A. S.; Mrsa, V.; Teparic, R. Surface display-An alternative to classic enzyme immobilization. *Catalysts* **2019**, *9*, No. 728.
(37) Chen, L.; Holmes, M.; Schaefer, E.; Mulchandani, A.; Ge, X. Highly active spore biocatalyst by self-assembly of co-expressed anchoring scaffoldin and multimeric enzyme. *Biotechnol. Bioeng.* **2018**, *115*, 557−564.
(38) Fernandez-Pacheco, P.; Arevalo-Villena, M.; Bevilacqua, A.; Corbo, M. R.; Perez, A. B. Probiotic characteristics in *Saccharomyces cerevisiae* strains: Properties for application in food industries. *LWT* **2018**, *97*, 332−340.
(39) Neiman, A. M. Prospore membrane formation defines a developmentally regulated branch of the secretory pathway in yeast. *J. Cell Biol.* **1998**, *140*, 29−37.
(40) Shi, L. B.; Li, Z. J.; Tachikawa, H.; Gao, X. D.; Nakanishi, H. Use of yeast spores for microencapsulation of enzymes. *Appl. Environ. Microbiol.* **2014**, *80*, 4502−4510.
(41) Lipke, P. N.; Ovalle, R. Cell wall architecture in yeast: New structure and new challenges. *J. Bacteriol.* **1998**, *180*, 3735−3740.
(42) Bemena, L. D.; Mukama, O.; Neiman, A. M.; Li, Z. J.; Gao, X. D.; Nakanishi, H. *In vitro* reconstitution of the yeast spore wall dityrosine layer discloses the mechanism of its assembly. *J. Biol. Chem.* **2017**, *292*, 15880−15891.
(43) Li, Z. J.; Liu, X. X.; Nakanishi, H.; Gao, X. D. Encapsulation of mannose-6-phosphate isomerase in yeast spores and its application in L-ribose production. *J. Agric. Food Chem.* **2020**, *68*, 6892−6899.
(44) Zhang, H. N.; Tachikawa, H.; Gao, X. D.; Nakanishi, H. Applied usage of yeast spores as chitosan Beads. *Appl. Environ. Microbiol.* **2014**, *80*, 5098−5105.
(45) Li, Z. J.; Li, Y.; Duan, S. L.; Liu, J.; Yuan, P.; Nakanishi, H.; Gao, X. D. Bioconversion of D-glucose to D-psicose with immobilized D-xylose isomerase and D-psicose 3-epimerase on *Saccharomyces cerevisiae* spores. *J. Ind. Microbiol. Biot.* **2015**, *42*, 1117−1128.
(46) Pechsrichuang, P.; Yoohat, K.; Yamabhai, M. Production of recombinant *Bacillus subtilis* chitosanase, suitable for biosynthesis of chitosan-oligosaccharides. *Bioresour. Technol.* **2013**, *127*, 407−414.
(47) Zhou, J.; Harindintwali, J. D.; Yang, W.; Han, M.; Deng, B.; Luan, H.; Zhang, W.; Liu, X.; Yu, X. Engineering of a chitosanase fused to a carbohydrate-binding module for continuous production of desirable chitooligosaccharides. *Carbohydr. Polym.* **2021**, *273*, No. 118609.
(48) Álvarez-Cao, M.-E.; Cerdán, M. E.; González-Siso, M. I.; Becerra, M. Optimization of *Saccharomyces cerevisiae* α-galactosidase production and application in the degradation of raffinose family oligosaccharides. *Microb. Cell Fact.* **2019**, *18*, No. 172.
(49) Cheng, H. L.; Zhao, R. Y.; Chen, T. J.; Yu, W. B.; Wang, F.; Cheng, K. D.; Zhu, P. Cloning and characterization of the glycoside hydrolases that remove xylosyl groups from 7-beta-xylosyl-10-deacetyltaxol and its analogues. *Mol. Cell Proteomics* **2013**, *12*, 2236−2248.
(50) Zou, S.; Chen, T. J.; Li, D. Y.; Fan, S.; Yang, Z. Y.; Zhu, P. LXYL-P1-2 immobilized on magnetic nanoparticles and its potential application in paclitaxel production. *Electron. J. Biotechnol.* **2021**, *50*, 10−15.
(51) Nampally, M.; Moerschbacher, B. M.; Kolkenbrock, S. Fusion of a novel genetically engineered chitosan affinity protein and green fluorescent protein for specific detection of chitosan *in vitro* and *in situ*. *Appl. Environ. Microbiol.* **2012**, *78*, 3114−3119.
(52) Li, B. J.; Wang, H.; Gong, T.; Chen, J. J.; Chen, T. J.; Yang, J. L.; Zhu, P. Improving 10-deacetylbaccatin III-10-beta-O-acetyltransferase catalytic fitness for Taxol production. *Nat. Commun.* **2018**, *9*, No. 16221.
(53) Yang, L.; Chen, T. J.; Wang, F.; Li, L.; Yu, W. B.; Si, Y. K.; Chen, J. J.; Liu, W. C.; Zhu, P.; Gong, W. Structures of β-glycosidase LXYL-P1-2 reveals the product binding state of GH3 family and a specific pocket for Taxol recognition. *Commun. Biol.* **2020**, *3*, No. 22.
(54) Qi, B.; Luo, J.; Wan, Y. Immobilization of cellulase on a core-shell structured metal-organic framework composites: Better inhibitors tolerance and easier recycling. *Bioresour. Technol.* **2018**, *268*, 577−582.
(55) Fang, G.; Chen, H.; Zhang, Y.; Chen, A. Immobilization of pectinase onto Fe_3O_4@SiO_2-NH_2 and its activity and stability. *Int. J. Biol. Macromol.* **2016**, *88*, 189−195.
(56) Wang, Y.; Chen, D.; Wang, G.; Zhao, C.; Ma, Y.; Yang, W. Immobilization of cellulase on styrene/maleic anhydride copolymer nanoparticles with improved stability against pH changes. *Chem. Eng. J.* **2018**, *336*, 152−159.

https://doi.org/10.1021/acs.jafc.2c01983
J. Agric. Food Chem. 2022, 70, 7479−7489

(57) Suman, S. K.; Patnam, P. L.; Ghosh, S.; Jain, S. L. Chicken feather derived novel support material for immobilization of laccase and its application in oxidation of veratryl alcohol. *ACS Sustainable Chem. Eng.* **2019**, *7*, 3464−3474.

https://doi.org/10.1021/acs.jafc.2c01983
J. Agric. Food Chem. 2022, 70, 7479−7489